Measuring Methane Production of Cattle in a Semi-Closed Environment

Sarah Popenhagen, Danylo Sovgut, Yuchen Wang, and Emily Zhang

University of Illinois at Urbana-Champaign
PHYS 398 DLP

December 6, 2019

Abstract

The production of methane gas by cattle presents a significant environmental problem. Methane gas contributes to global warming through the greenhouse effect. The methane production of individual herds of cattle can be influenced by many factors, including diet and genetics.

The purpose of this study is to develop and present a method of effectively and affordably measuring the relative methane production of cattle using a microcontroller board and compatible environmental sensors. Using this method, members of the industry can monitor the impact of their cattle on the environment at a low cost without changes to the routine of the herd.

Results from our sensors clearly show a difference in gas concentration between an environment with cattle and one without. Therefore, even with budget sensors, the measurement of the gas is possible. The results from our method can be used to minimize the methane emissions of a herd by comparing emissions during periods of differing diet and making changes accordingly.

1 Background Information and Introduction

Cattle are significant producers of the greenhouse gas methane. Ruminants such as cattle have a specialized stomach containing methanogenic bacteria. The bacteria ferment food before digestion, producing and releasing methane gas. (Patra, 2017)

Like other greenhouse gases, atmospheric methane absorbs and emits radiation and contributes to the greenhouse effect, a process which warms Earth's surface. Levels of greenhouse gases have risen drastically in recent history due to human activity such as the burning of fossil fuels and large-scale deforestation. (EPA, 2019)

The results of the corresponding increase in the greenhouse effect are difficult to predict. Likely consequences include increases in average world temperature and sea level, both of which have the potential to be disastrous for society if left unchecked. While it is one of the least abundant greenhouse gases, methane is nevertheless an important factor as it has 32 times the effect on global warming as carbon dioxide, by mass. (EPA, 2017)

Methane gas accounts for 10 percent of global warming. With an estimated 1.5 billion cattle worldwide, the cattle industry accounts for 40 percent of the world's methane output. A cow does on overage release between 70 and 120 kg of methane per year (TC, 2008). Numerous studies are currently attempting to discover new ways of mitigating the impact of cattle on the atmosphere. Advances in cattle nutrition and genetics in recent years have shown it is possible to reduce the amount of methane cattle produce with changes to herd genetics and diet. (K. A. Johnson, 1995)

In this study, we will be developing an effective and affordable method of measuring the methane production of cattle. This method can be used by cattle owners to evaluate the emissions of their herds and potentially reduce said emissions. Our trial was conducted on a group of steers at the University of Illinois Beef and Sheep Field Research Laboratory in Urbana, Illinois. Pictured in Figure 1 are three young steers similar to those in our study.

Figure 1: Photo of three young steers. From left to right: Zobrist, Javy, and Bryzzo. Image owned by Sarah Popenhagen.

2 Materials

2.1 Arduino Mega 2560

The Arduino Mega 2560 microcontroller is the primary device used in the project. It is based on Atmel's ATmega2560 and is used to execute our programs and collect data.

The ATmega2560 includes an 8-bit microcontroller, 256 kB programmable flash memory, 8 kB RAM, 4 kB EEPROM, and **S**erial **P**eripheral **I**nterface (SPI). The microcontoller is suitable for low electrical power and less computationally extensive applications. The flash memory stores the Arduino executable program and is non-volatile, meaning information is stored and not lost when power is turned off. RAM is volatile (its data is lost when power is turned off) and is used to store variables.

As shown in Figure 2, the Arduino Mega 2560 has 16 analog-to-digital converter channels, multiple sets of **I**nter-**I**ntegrated **C**ircuit (I^2C) ports, and a reset button. I^2C is a communication protocol that allows multiple "slave" digital integrated circuits (the environmental sensors we use in this project) to communicate with a "master". It uses a **S**erial **C**lock **L**ine (SCL) and a **S**erial **D**at**A** line (SDA) to communicate between the devices (Atmel, 2014).

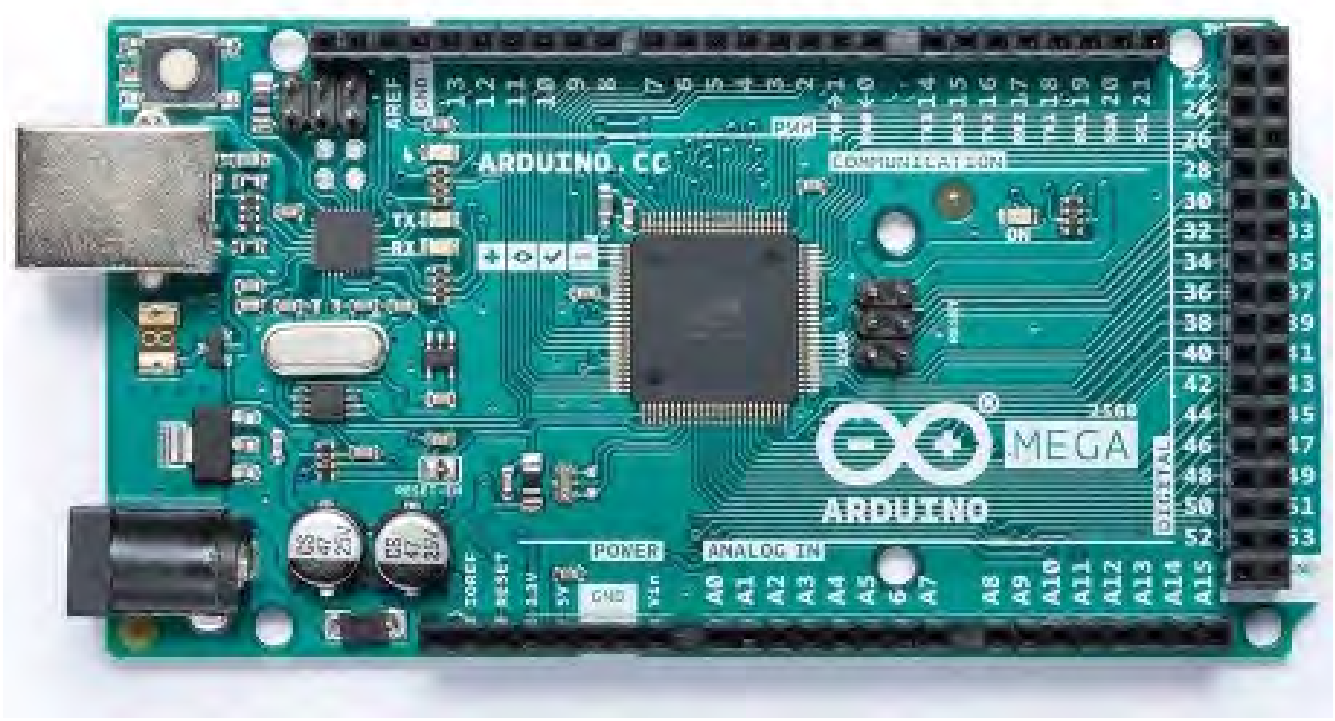

Figure 2: The Arduino Mega 2560. Retrieved from Arduino (2019).

2.2 BME680

The BME680, shown in Figure 3, is a multipurpose environmental sensor which measures temperature, atmospheric pressure, humidity, volatile organic compound (VOC) concentrations, and approximate altitude.

Within 0 °C to 65 °C, 300 hPa to 1100 hPa, and 10% to 90% relative humidity, the manufacturer guarantees error within 0.5 °C. The VOC sensor does not recognize carbon dioxide. The altitude

measurement requires current atmospheric pressure at sea level and provides the approximate altitude in meters (Bosch, 2017).

We use the temperature data from the BME to monitor the temperature of the environment while the other sensors are taking data.

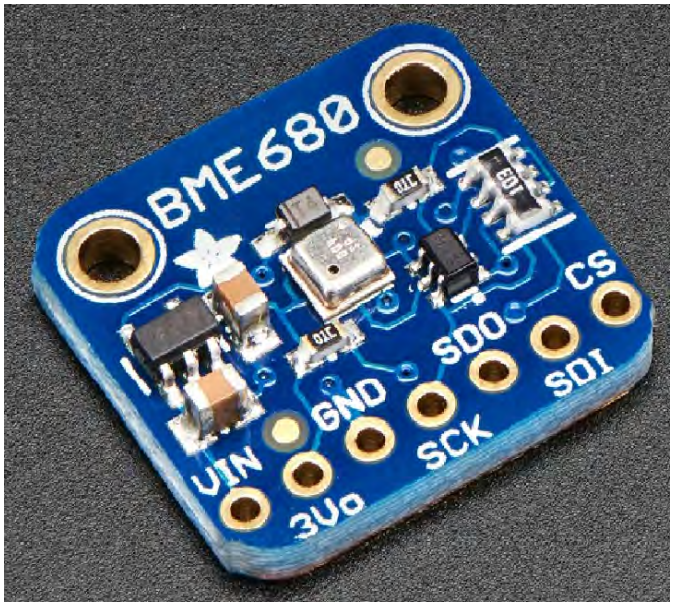

Figure 3: BME680. We used the I^2C Clock and **S**erial **D**ata **I**n (SDI) pins visible in the image to connect to the SCL and SDA I^2C lines, respectively. Figure adapted from Adafruit (2019).

2.3 Gas Sensors

We use 5 different sensors, shown in Figure 8, to measure the gas emissions from cattle. Their names and target gases are listed in the table in Figure 6. The primary purpose of our sensors is to detect high concentration of the corresponding gasses (for instance, the MQ-4 methane sensor is used to detect a methane leak in a household kitchen). The sensitive material in all of the sensors is tin oxide; its conductivity increases as the concentration the corresponding target gas increases. We connect each sensor to a 10kΩ resistor (labeled R_L in Figure 4) and measure the voltage across the 10kΩ resistor as shown below. Therefore, our measurement increases as concentration increases. In Figure 4, the sensor is represented by the circle in the center of the diagram. There are two separate circuits: one to heat the sensors' internal heating resistors and one to connect each of the 10kΩ resistors and gas sensors in series. This allows us to record the relevant voltage value, represented in the figure by V_{RL}.

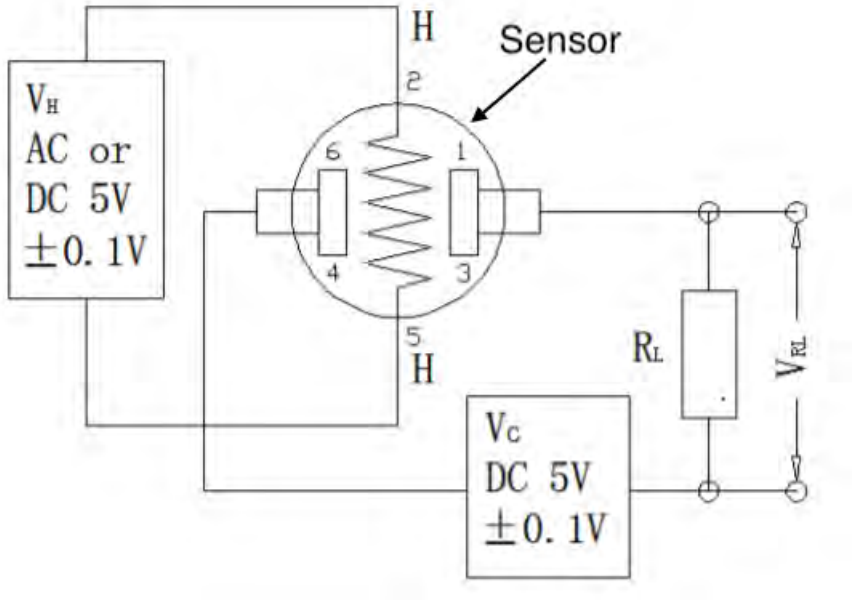

Figure 4: The circuits used to connect the sensors. The circuits are identical for all five sensors. Figure retrieved from the manual of alcohol sensor MQ-3B (Zhe, 2015a).

2.3.1 Sensor Structure

A diagram of the structure of the sensors is shown in Figure 5. Each sensor has six pins. The pins labeled with the same letter (A, B, or H) are connected internally. The structure of the sensors are identical, but their differing working mechanisms are detailed in the following sections (Zhe, 2015a).

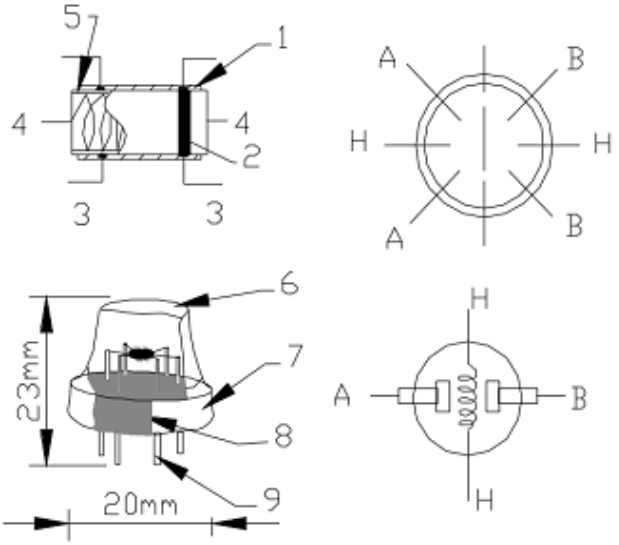

	Parts	Materials
1	Gas sensing layer	SnO_2
2	Electrode	Au
3	Electrode line	Pt
4	Heater coil	Ni-Cr alloy
5	Tubular ceramic	Al_2O_3
6	Anti-explosion network	Stainless steel gauze (SUS316 100-mesh)
7	Clamp ring	Copper plating Ni
8	Resin base	Bakelite
9	Tube Pin	Copper plating Ni

Figure 5: This figure shows the internal structure of the alcohol sensor MQ-3B in detail. The structure is the same for all five sensors.

Sensor	Target Gas
MQ-3B	Alcohol
MQ-4	Methane
MQ-6	Liquified Petroleum Gas
MQ-7B	Carbon Monoxide
MQ-8	Hydrogen

Figure 6: This table summarizes types of sensors we used.

2.3.2 Reducing Gas Sensors

When a reducing gas touches the tin oxide layer in the sensor, it donates electrons. This layer acts as an n-type metal oxide semi-conductor. The majority of charge carriers on the sensing layer are electrons. Contact with electron donors (such as ethanol) will increase the conductivity of this layer (Negri, 2007). See Figure 7 for a visualization of this process.

The specific target gas of the MQ-3B is ethanol, however our empirical attempts demonstrated that it also reacts to isopropyl alcohol. Theoretically, all vaporized alcohols are reducing gases and thus the sensor should react to them (Zhe, 2015a). The heavier the molecular weight, however, the less sensitive the sensor.

The target gas of the MQ-7B is carbon monoxide. The manufacturers do not provide detailed information on the design of the sensors, but we disassembled one of our spares and found a solenoid wrapped in a membrane. We assume that the membrane isolates the solenoid from all but the target gas.

2.3.3 Oxidizing Gas Sensors

Oxidizing gases treat the tin oxide layer as a p-type semiconductor. The majority charge carriers here are the vacancies in the crystal lattices. The gas will take more electrons and create more vacancies, thus will lead to an increase in conductivity.

The target gases of the MQ-4, MQ-6, and MQ-8 sensors are methane, liquified petroleum gas, and hydrogen, respectively.

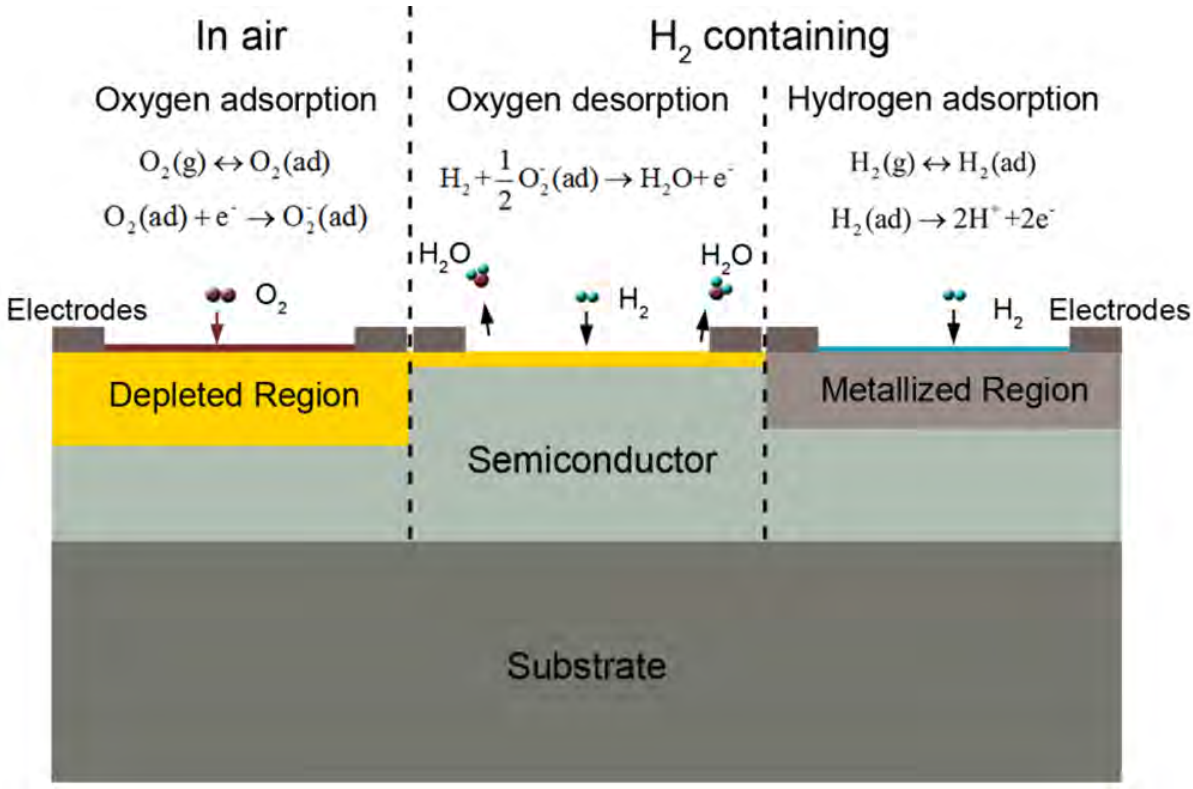

Figure 7: This is a cross section of a generic hydrogen sensor. We hypothesize that our sensors function similarly to the one shown in this figure. The semiconductor absorbs oxygen gas molecules in the air. Oxygen extracts electrons from the layer and forms a depleted region. Hydrogen gas provides electrons to the metallized region. The oxygen ions and hydrogen ions react with each other and produce water molecules and electrons. The electrons produced decrease the resistance of the semiconductor. Figure retrieved from Gu et al. (2012).

2.4 Additional Components

We used a **L**iquid **C**rystal **D**isplay (LCD) to display messages about the activity of the device in the field. The LCD displays a message when the device records data without any issue, or an error message otherwise. It also prints out messages indicating whether the device encountered a problem saving the data. We used an SD card breakout board to write and save data to SD cards. Additionally, we used a keypad to communicate with the device without connecting to a computer, a DS3231 **R**eal **T**ime **C**lock (RTC), shown in Figure 9, to record the date and time of each measurement, and an INA219 current sensor to monitor the current draw of the device. Several of these components are visible in Figures 9 and 10.

Our SD breakout board, LCD, and keypad are all connected to general purpose input/output pins. We used 5 **A**nalog-to-**D**igital **C**onverter (ADC) channels for our gas sensors and an I^2C for the BME680, DS3231 RTC, and INA219.

In early stages of the experiments, all the devices mentioned were connected to breadboards. When conducting measurements in the barn, we used printed circuit boards designed by Professor George Gollin, to which we soldered all our devices. Figure 11 shows a fully assembled device. Some components, such as the BME680 and most of the individual gas sensors, were used primarily for cross-checking and calibration. The BME680's temperature measurements proved to be invaluable

in troubleshooting sensor malfunctions.

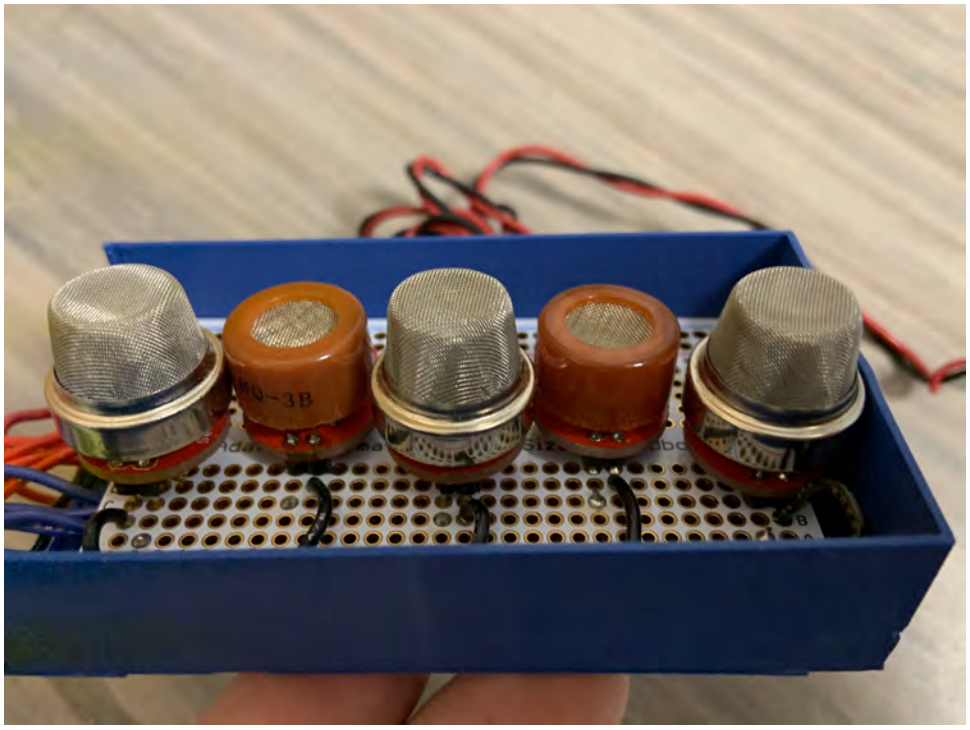

Figure 8: These are our gas sensors, which are connected to the Arduino.

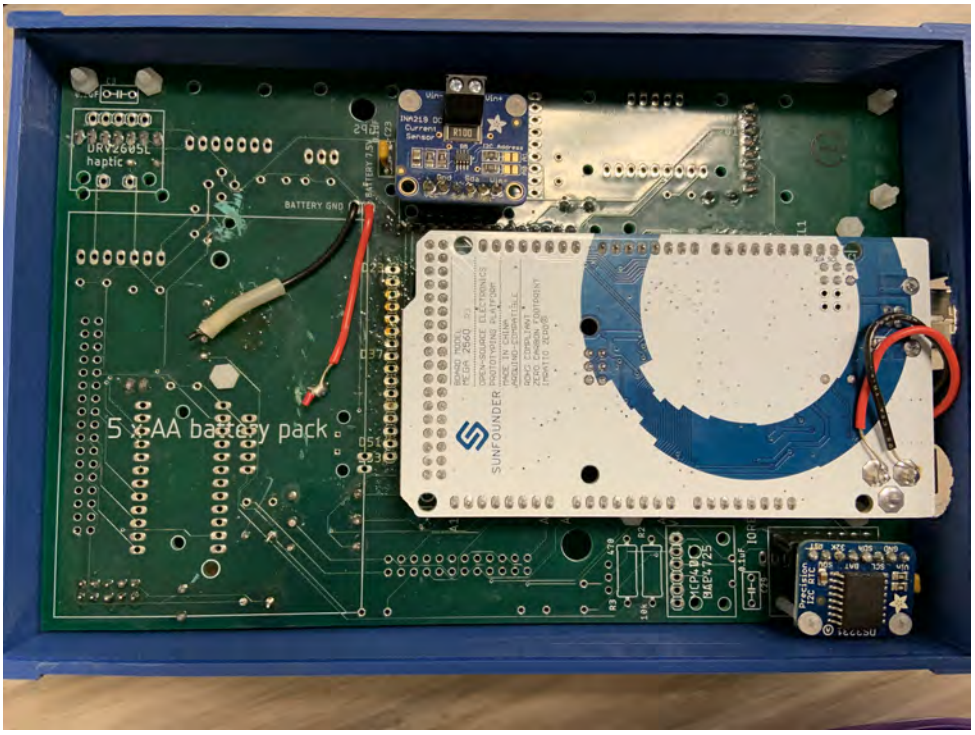

Figure 9: This figure shows our device without the back cover. You can see a Sunfounder (microcontroller board identical to Arduino), a real time clock, and an INA219 Current Sensor.

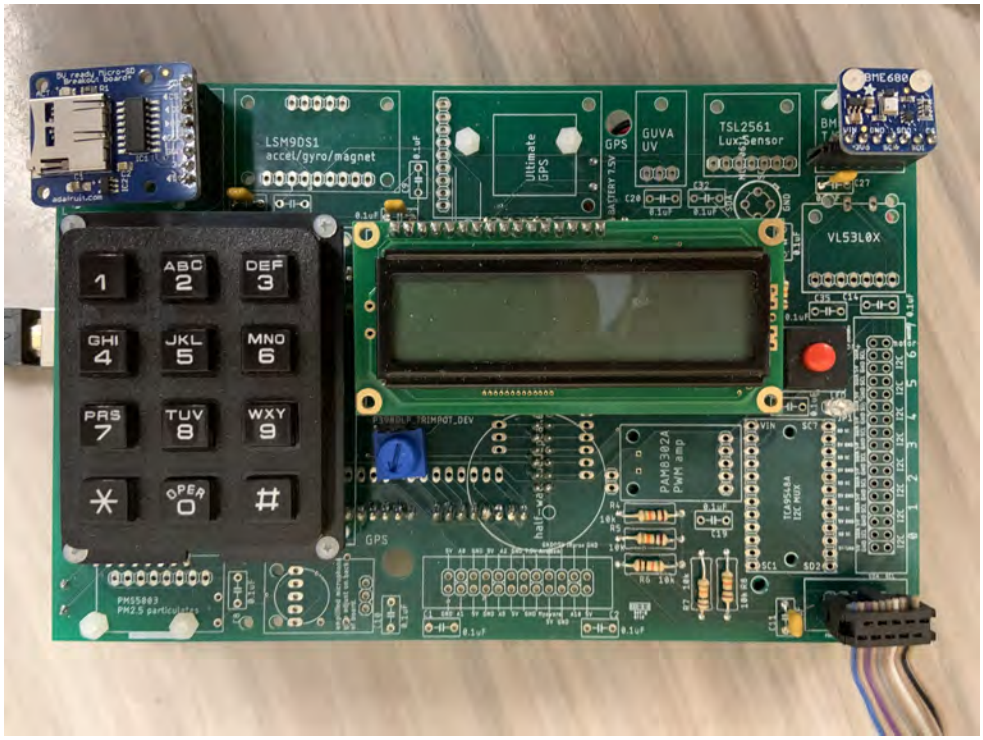

Figure 10: This figure shows the front of our device. Visible are: an LCD screen and a blue variable resistor underneath to control brightness, a keypad, an SD Card breakout on the top left, a BME680 sensor on the top right, and the connection to the gas sensors on the bottom right.

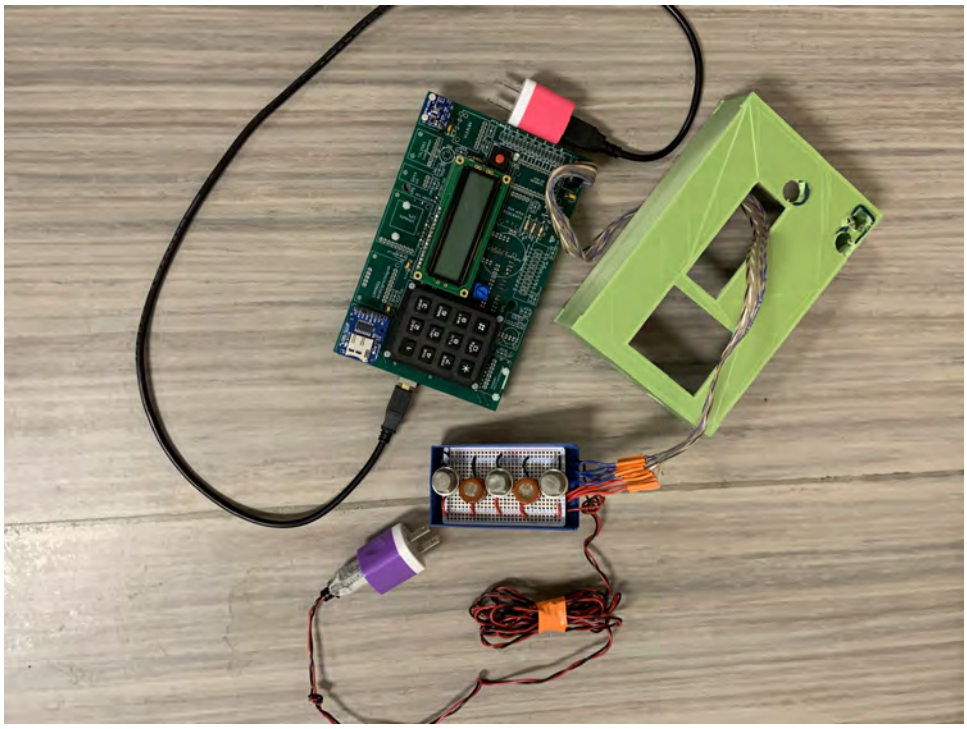

Figure 11: This shows our whole device. The Arduino and the heating elements of the sensors are powered by separately. The sensors are connected to the Arduino and rest of the components by a ribbon cable, which allows greater mobility for the sensors.

3 Methods

To ensure the accuracy of the data, we ran all the sensors for 48 hours before taking any data. This "burn-in" time was advised by the manufacturer of the sensors. Once the sensors were burned in, we cross-calibrated our devices with simultaneous data taken with all four devices in an environment without any methane sources. Finally, we set up our devices at the University of Illinois at Urbana-Champaign Beef and Sheep Field Research Laboratory. We set up two devices in the vicinity of the steers to take data measurements and two devices away from the steers to take control measurements. This placement was chosen to ensure duplicates of the data and the control measurements in case of device failure or sensor malfunction. This experimental set-up allows us to measure relative concentration of methane gas both near and far from cattle. Figures 12-16 show the placement of the sensors.

Figure 12: The red arrows point to one of our devices, placed on the wooden block directly over the steers. Another device is directly behind the blue device shown on the picture. A second device is set up at the same wooden block and can be seen in Figure 13

Figure 13: Our devices, placed on the wooden block also pictured in Figure 12.

Figure 14: This picture shows the room in which we placed our devices. The red arrows indicate the location of our sensors. There were 6 steers in the stalls at the time of the experiment.

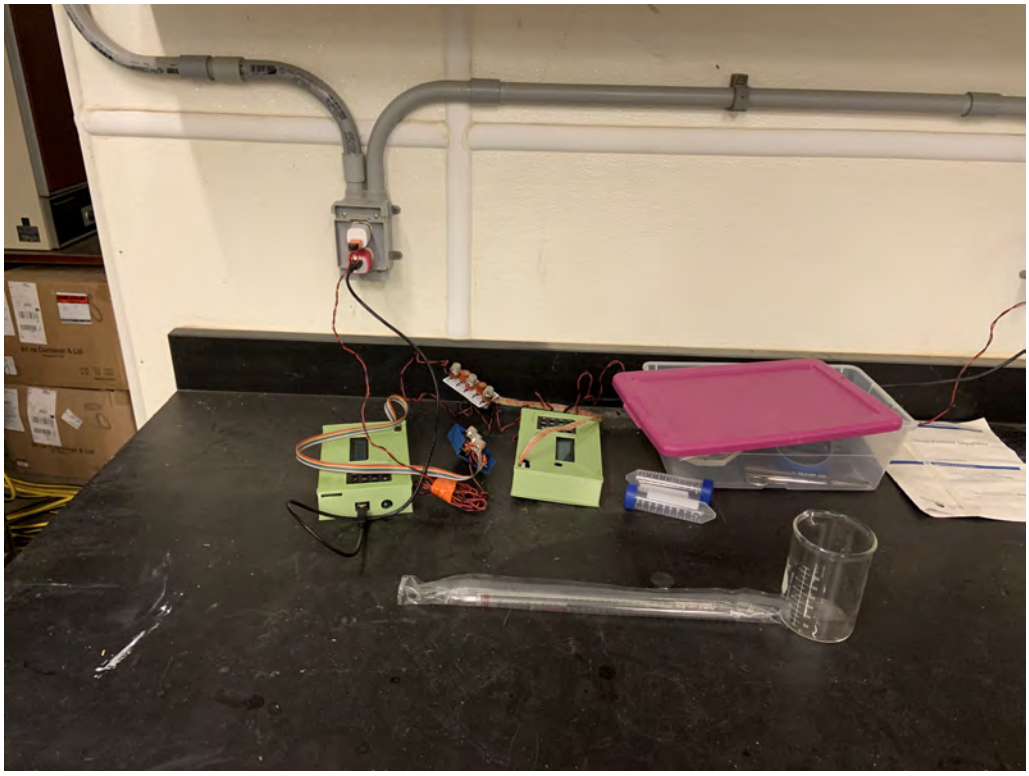

Figure 15: This picture shows two control devices, placed away from the steers in a separate room.

Figure 16: A door from the control room is open to the room with the stalls so some methane could also travel to the control room. However, we have compared the barn control sample with the calibration sample set-up in the lab away from the steers for added clarity.

Two of our devices are placed directly over the steers to maximize the amount of emissions detected. The barn is air conditioned and heated. Six specially trained steers, which researchers use for their experiments, are tied to the individual stalls near our devices. This barn is advantageous because the temperature is controlled. However, the air inside the barn is constantly circulated which removes a significant amount of methane and other emitted gases. To account for this inconsistency, we set up two devices as a control in a connected room. Devices were put in the enclosed barn as opposed to a larger, open-air barn that was also available because the recommended operating temperature for these sensors is 21°C. This experiment was performed during the late fall in Illinois, where temperatures could fall below 0°C.

4 Calibration

4.1 Cross-Calibration

After the initial trials in the open barn, some of our gas sensors were damaged and could no longer produce accurate readings. However, the sensors that detect methane, the main interest of this study, were all intact. Therefore, we will only calibrate the methane sensors. Cross-calibration was achieved using measurements taken simultaneously by the sensors while all the devices were running in an area far from any significant sources of methane. After the first cross-calibration run, one of the files recorded was corrupted and we were unable to recover it. By the time we discovered the problem, one of the other sensors had been damaged and unable to record data. To resolve the issue, we completed another calibration run with the three working devices, intending to average the results. This proved unnecessary, as our results were nearly identical between runs. The method used to perform the cross-calibration is detailed below.

We began by taking the mean of the 80 measurements each sensor takes in the duration of one minute. The mean difference between the readings of an individual sensor and the average of all the sensors was then taken in order to calculate an offset for each individual sensor. These offsets were then used to calibrate the data taken at the barn. In the two calibration runs we completed, the devices varied similarly. One device was nearly identical to the average and thus did not require an offset.

Figure 17 shows the calibration data used to compute the offsets and the same data after cross-calibration. The fourth sensor (not displayed) was the most accurate of the four.

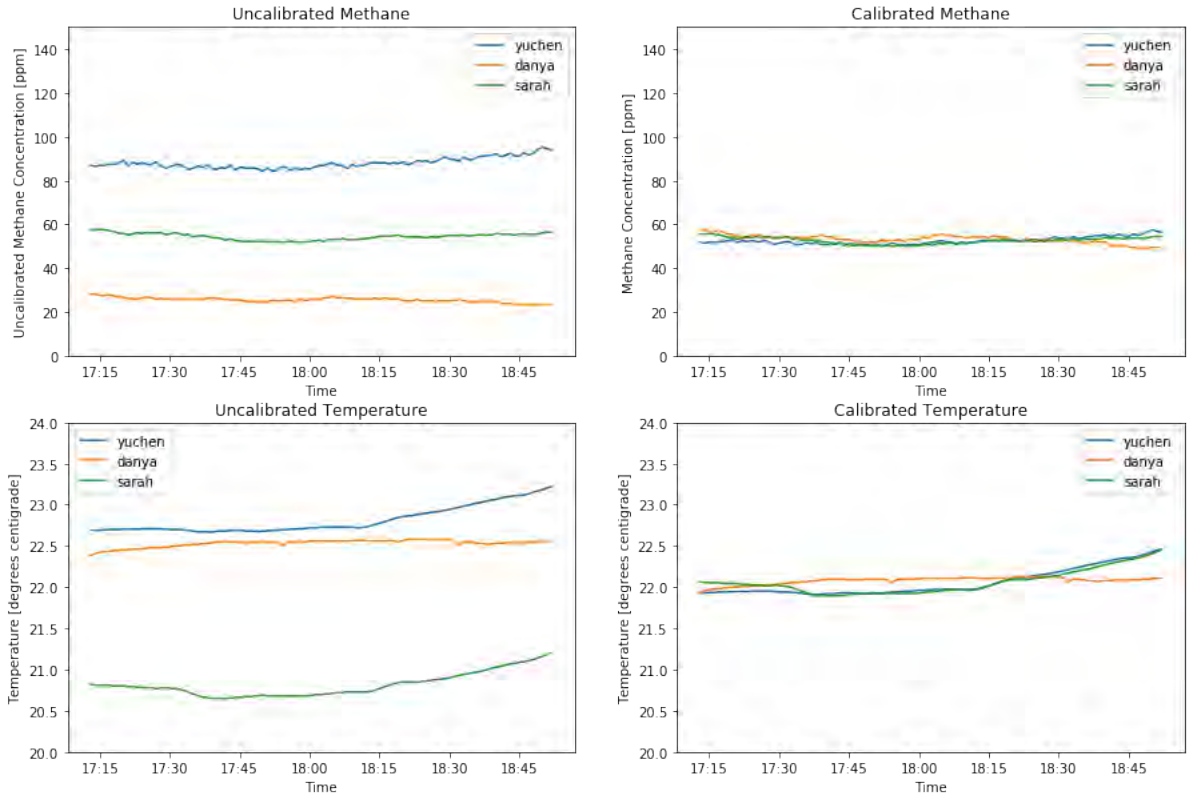

Figure 17: Calibration of methane and temperature measurements.

4.2 Temperature Dependence

We used the temperature measurements taken by the BME680 to check for temperature dependence on our gas concentration measurements. The dependence was found to be small, with a very slight increase in readings with increasing temperature. Within the temperature range of our measurements, the effect was negligible. We learned, however, that the readings of the sensors become extremely unreliable below 15°C.

4.3 Data Calibration

Our original plan was to gain access to the target gases of the sensors via chemistry labs and conduct sensor calibrations there. Unfortunately, we were not able to access labs that use these gases, making it necessary to use the manufacturer's data alone to convert and calibrate our measurements.

The manufacturer's data we used to generate calibration equations was based on the average measurements of many sensors. For each sensor, their plot only tells us that there is a nonlinear relationship between the voltage reading and the gas concentration. This introduces some uncertainty in our data.

For each sensor, we chose eight points from the sensitivity plot. Here are the curves provided by the manufacturer for each sensor and our calculated fit equations. When using gas concentration as the independent variable, to our surprise, second degree natural log functions were the best fit. The sensitivity curves are displayed in Figures 18-22.

The fact that we were only able to calibrate our sensors using the manufacturer's data did not hinder our experiment because the only gas emission of interest is methane and all of our methane sensors were performing correctly. Some of the other sensors were damaged enough that they could no longer read accurate data. Even though carbon monoxide was not of interest in this study, our sensors did report some interesting readings of carbon monoxide in the open barn when the carbon monoxide sensors were functioning correctly. This will be discussed in Section 6; the relevant data is displayed in Figure 26.

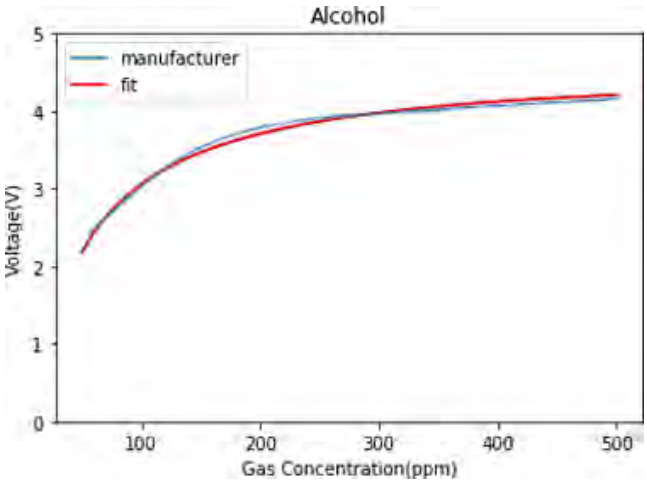

Figure 18: Sensitivity curves for alcohol sensor MQ-3B. Adapted from Zhe (2015a).

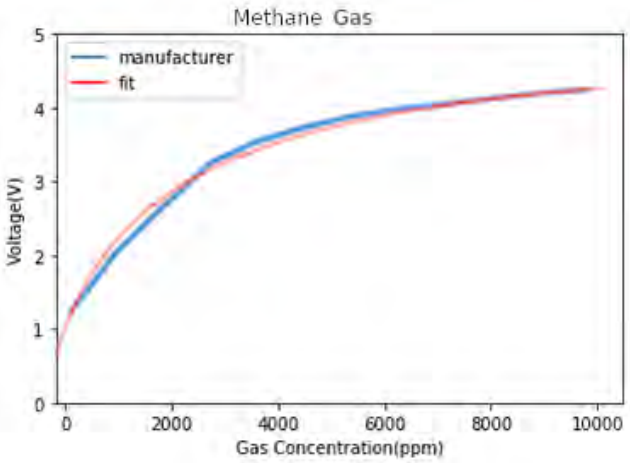

Figure 19: Sensitivity curves for methane sensor MQ-4. Adapted from Zhe (2015b).

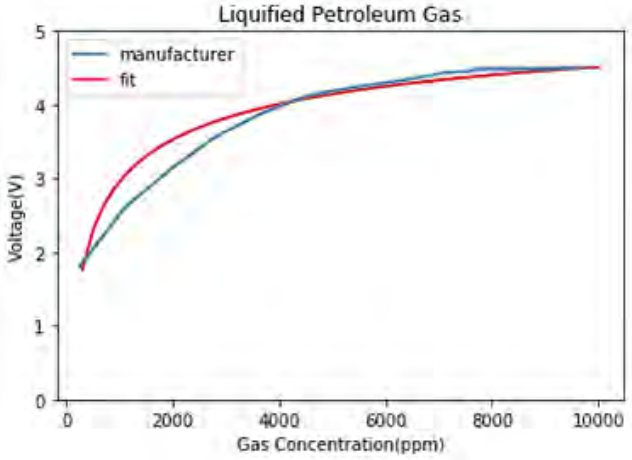

Figure 20: Sensitivity curves for liquefied petroleum gas sensor MQ-6. This fit is worse than the rest, but we did not use LPG measurements so it is of low importance. Adapted from Zhe (2015c).

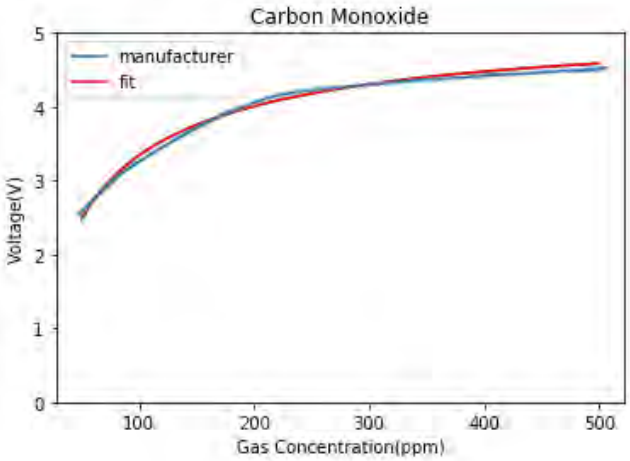

Figure 21: Sensitivity curves for carbon monoxide sensor MQ-7B. Adapted from Zhe (2018).

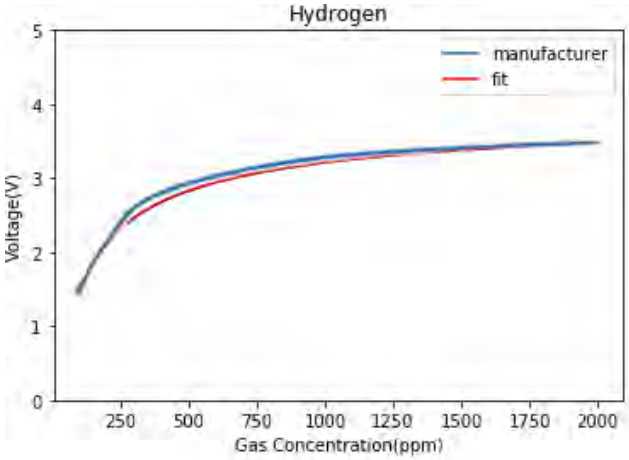

Figure 22: Sensitivity curves for hydrogen sensor MQ-8. Adapted from Zhe (2015d).

4.4 Conversion of Raw Data to Gas Concentration

The gas sensors report values between 0 to 1023 based on the voltage difference they experience. This value can be converted to voltage easily by:

$$\text{Voltage} = \frac{5x}{1023}$$

Since the manufacturer connects a 4.7kΩ resistor in series with each sensor while we use 10kΩ resistors, we must convert our measured voltage to the value which it would be if we had used a 4.7kΩ resistor. We assume that at the same gas concentration, the heat resistances of our sensors are the same as the manufacturer's.

As what we measure is the voltage, we want equations that can tell us what concentrations in unit of molecule parts per million (ppm) each voltage value corresponds to. Therefore, we generated five equations for our five sensors with V being our voltage readings:

$$\begin{aligned}
\text{Alcohol gas concentration [ppm]} &= 0.13645\exp^2(V) - 2.9911\exp(V) + 80.701 \\
\text{Methane gas concentration [ppm]} &= 24.557414714\exp^2(V) - 63.98130888\exp(V) + 43.36546982 \\
\text{LPG gas concentration [ppm]} &= 1.103\exp^2(V) + 6.24971V + 377.95 \\
\text{Carbon Monoxide concentration [ppm]} &= 0.061349\exp^2(V) - 1.5935\exp(V) + 84.246 \\
\text{Hydrogen gas concentration [ppm]} &= 2.989\exp^2(V) - 45.151\exp(V) + 320.298
\end{aligned}$$

5 Software

5.1 Data Acquisition Program

Our **D**ata **Ac**q**u**isition Program (DAQ) checks if all devices are functioning before it starts to record data. Once it starts recording, the DAQ initializes a new CSV file in the SD card and begins to record data from the RTC, the BME680, and all five gas sensors. It stops recording and saves the file upon the user's request. The DAQ is divided into two phases: setup and recording.

During the setup phase, the DAQ begins by initializing the hardware. It then checks whether the RTC, the SD card and the BME680 are intact and responding. If any of the three are not fully functional, the LCD prints a message identifying the faulty device. If all devices are functioning, the DAQ opens a CSV file in the SD card and moves to the recording phase.

During the recording phase, the DAQ saves the following information in the CSV file: the current date and time from the RTC, temperature, pressure, humidity, gas resistance, and altitude readings from the BME680, and analog data values from the alcohol, methane, LPG, carbon monoxide, and hydrogen gas sensors. The sensors report values between 0 to 1023 based on the voltage difference they experience. The DAQ saves the file after each cycle. If the user terminates the device during a cycle, everything recorded before this cycle is saved. If the user prefers to include the current cycle, DAQ will save the file after its completion upon the user's request. If the user takes the SD card out for data collection, the LCD will report the absence of the SD card and break the loop.

5.2 Data Analysis Program

Our **D**ata **A**nalysis **P**rogram (DAP), written in Python, visualizes and converts data collected by our devices. The Analog Digital Converter of the Arduino is a 10 bit converter, which means there are 1024 distinct values that it can record. The reference voltage is 5 Volts, therefore our DAP converts the ADC input to the voltage on our sensors using the equation shown in section 4.3. The DAP then converts the voltages into gas concentrations in ppm as described in the calibration section. Our DAP then applies the cross-calibration offsets described in section 4.3 and plots the results versus time. The DAP creates an additional plot of the difference between the measurement and the control. Finally, the DAP calculates and prints the average measurement, average control, and the difference of the two in parts per million.

6 Results

During preliminary data collection, we set up two devices in the enclosed barn described in section 3, and two devices in an open-air barn. In each of the locations, one device was placed in the vicinity of the cattle and the other device was placed away from the cattle as control. However, due to extreme weather conditions, our devices did not perform as well as we anticipated. Some sensors were damaged and therefore malfunctioned, most likely due to extreme low temperatures and physical movement of the sensors during transportation. Some connections between our devices and the power supply were broken and some of the devices were permanently damaged. After repairing our devices and carefully calibrating our sensors, we decided to set up all four devices in the enclosed barn to avoid additional damage to the sensors and ensure the accuracy of our data. We placed two devices on top of the stall and two devices away from the cattle in case one or more sensors on a certain device were to malfunction.

The average concentration of methane measured above the stall was calculated to be 178.1 ppm, while the average control measured was 52.97 ppm. The difference in concentration due to proximity to the cattle was 125.13 ppm.

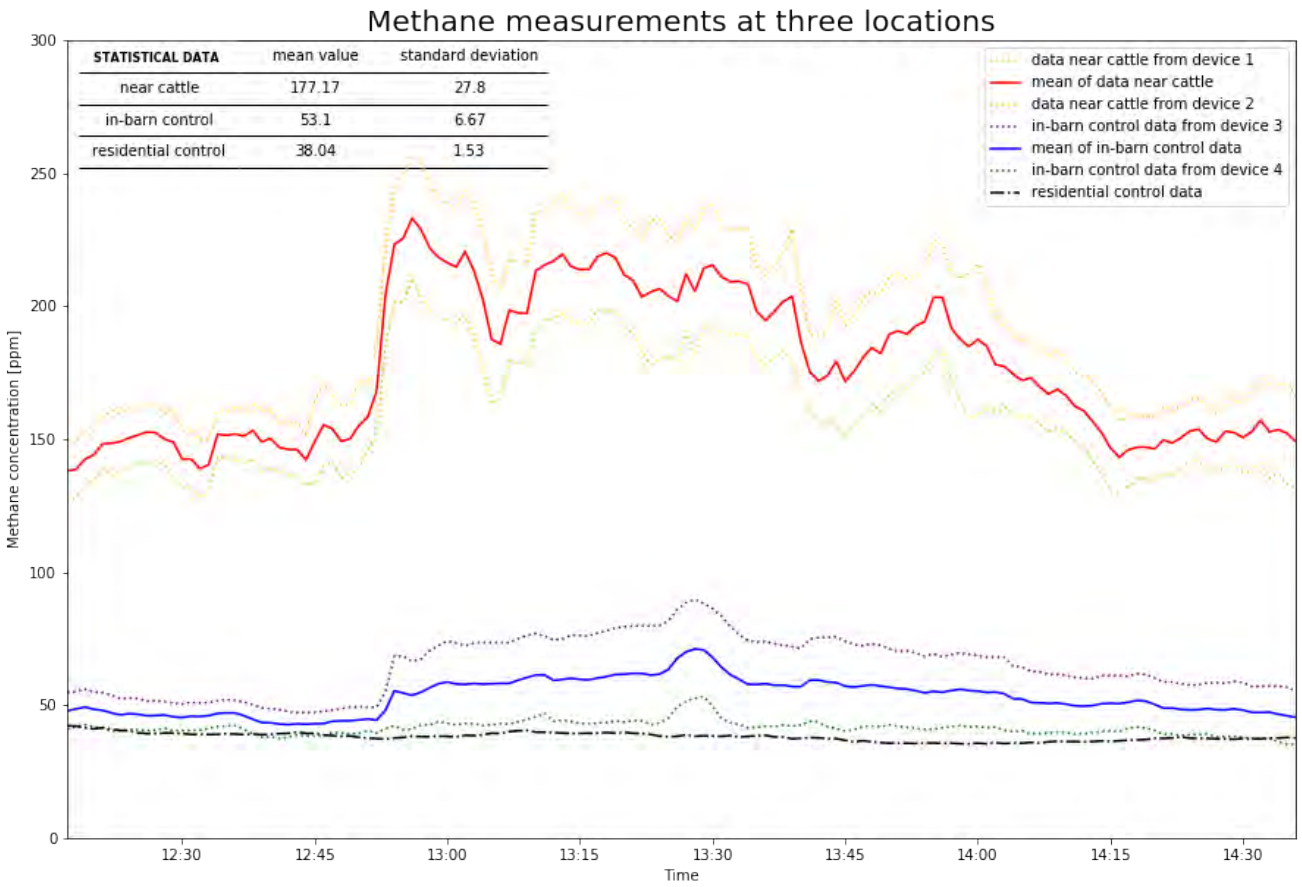

Figure 23: Measured methane levels at three locations: near the cattle, a separated room in the barn, and an empty room in an apartment. The residential control data was taken for the same duration of time and at the same temperature, but not taken on the same day as the sets of data from the barn, which were taken simultaneously.

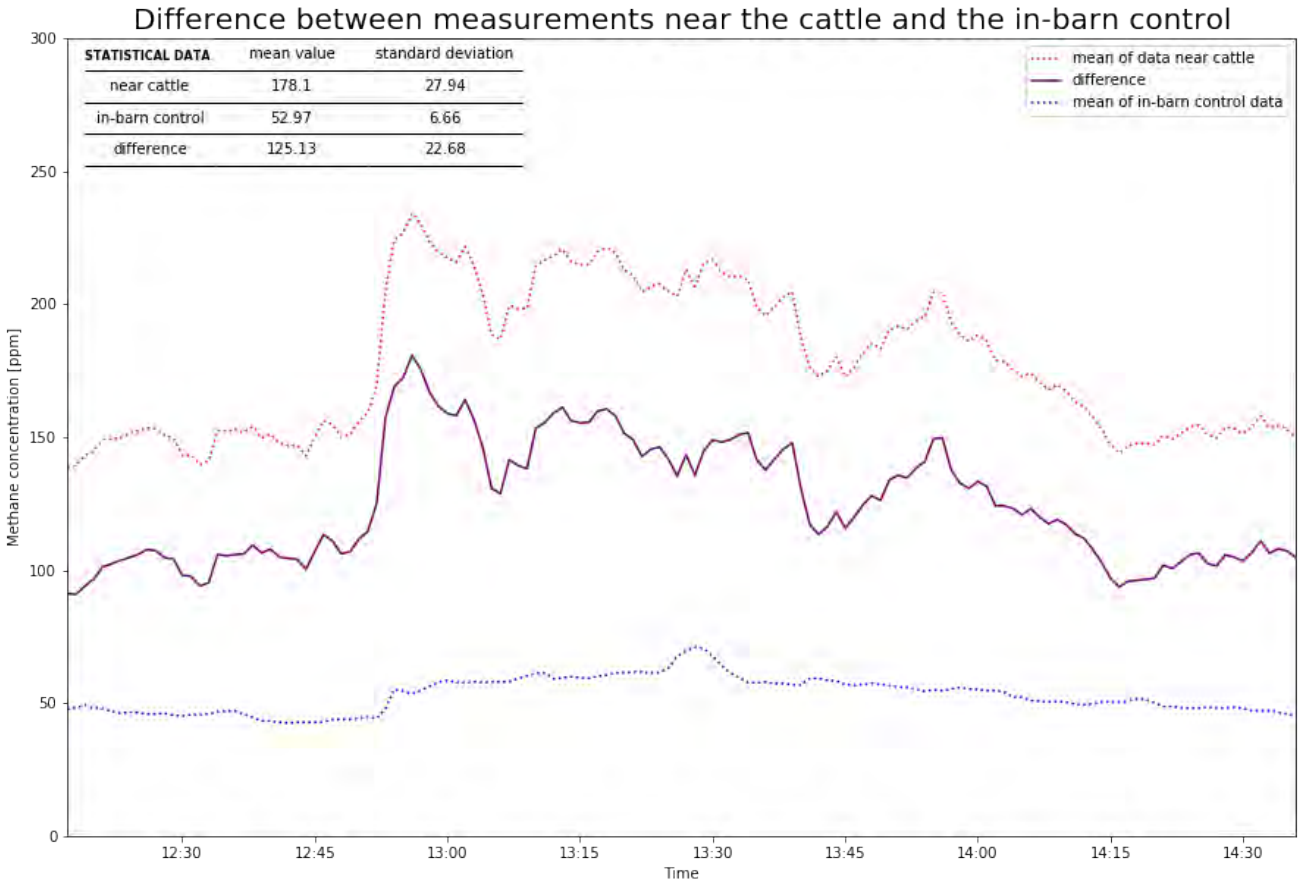

Figure 24: Difference between methane measurements taken near the cattle and the in-barn control. Measurements were taken simultaneously.

In order to visualize the results, we've plotted curves to present our data, shown in Figures 23 and 24. Alongside the measurements from the barn, an additional control curve is plotted in Figure 23. This control curve (labeled 'residential control' in the figure) was taken at a different time than the others, but its measurements' change in time was negligible. The residential control was taken in an empty room of an apartment in the same temperature range as the measurements from the barn. It is clear from the figures that the concentration of methane is much higher near the cattle than away from the cattle. Additionally, the methane levels fluctuate significantly more at the barn than the residential location. This was expected, as the digestive systems of cattle do not produce methane at a constant rate. We also noticed that there has been a consistent concentration spike in methane around 1:00 p.m. everyday during our data collection. We spoke with the farm manager and learned that they extract ruminant fluid from the steers at 1:00 p.m. everyday. This procedure sufficiently explains the concentration spike, as ruminant fluid contains methanogenic bacteria.

During data collection in the open barn, our sensors reported readings of carbon monoxide spikes at the same times each day. We learned from the farm manager that the times correlated with the delivery of food for the cattle by truck. The rise in carbon monoxide was very likely exhaust from the truck idling inside the barn while the cattle were being fed.

7 Discussion

We can easily see from our data that cattle contribute a lot to methane emission. Of all the greenhouse gases, methane is one of the most effective at warming, and there are huge numbers of cattle producing it worldwide. From the following map, we can see that cattle are raised all across the United States, except for the deserts of the Southwest and some remote mountains in upper New York state and West Virginia.(Klein, 2014)

With the large number of cattle in the U.S. (see Figure 25), their methane production is too significant to be ignored. It is necessary that cattle owners evaluate the emission of their herds and do what they can to reduce methane emissions.

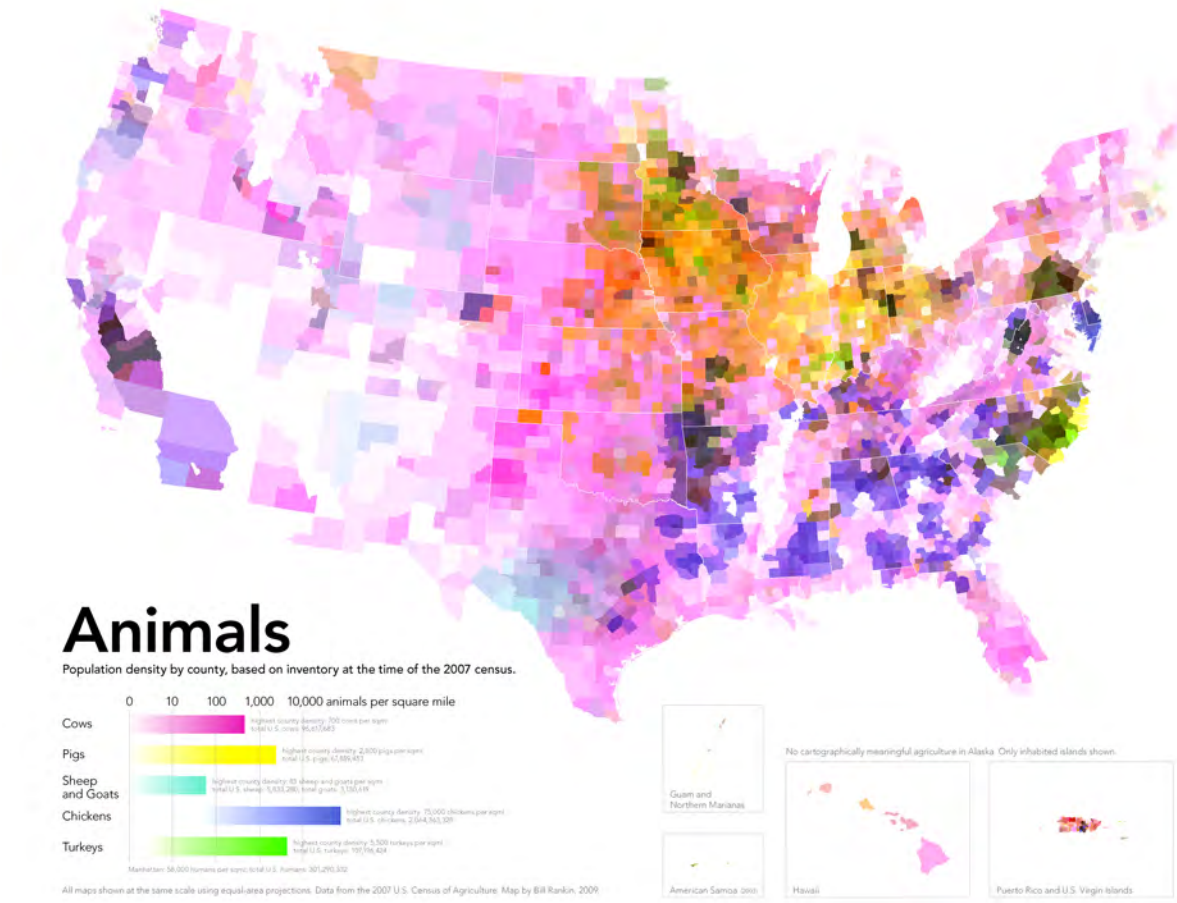

Figure 25: This figure shows the prominence of cattle and other livestock in the U.S.(Klein, 2014)

Our experiment uncovers the feasibility of running affordable and minimally intrusive emissions monitoring on small cattle farms. Traditionally, experiments that measure methane gas emissions from cattle use expensive equipment and dedicated space in barns. The cattle are kept in an enclosed box where the air is controlled and analyzed. The individual animals must be trained for multiple weeks to remain calm in an enclosed environment. Extra man hours are required for the moving of cattle to and from the environment, as well as for added complication to the farm's

feeding routine. Furthermore, the required equipment and sensors are too costly to be practical for most small farms. Methane detectors that analyze collected air samples can cost up to thousands of dollars and can be difficult to learn to operate. In contrast, our devices cost under 100 dollars and are easy to set up and use. The downside to our method is that it only measures relative methane concentration in the air of a barn, unlike the more expensive studies which measure the absolute production of methane by the cattle. For the majority of everyday purposes, however the relative concentration measurements are sufficient. Thus, the success of our experiment proves the feasibility of a simple and affordable method of measuring and monitoring the methane emissions of cattle.

Secondly, our experiment uncovers how suitable cheap gas sensors are for measuring comparatively low amounts of methane emissions from cattle. We discovered that the sensors are limited in their sensitivity, as the reducing gas sensors respond to all reducing gases, not just their target gas, and the oxidizing sensors likewise respond to all oxidizing gases. This phenomenon is shown in Figure 26. It can also be seen in our main results, as our control measurements were higher than expected based on the average concentration of methane in the atmosphere. These large measurements are likely due to the methane sensor responding to other oxidizing gases in addition to methane. Thus, while the cheap sensors are suitable for obtaining rough measurements of relative concentrations of gases known to be present, they are not suitable for identifying specific gases or precisely measuring concentrations.

Thirdly, our work shows the feasibility of measuring gas emissions in a semi-closed environment. Since, traditionally, these experiments are run in the expensive, fully-enclosed environments, the success of our experiment shows that a totally controlled environment is unnecessary for basic measurements. Farm owners can use these devices to monitor methane emissions in their barns without additional equipment or environments. Using the data from their farm, they could see whether changing the diet of their herd or their method of handling manure could help reduce emissions at their farm.

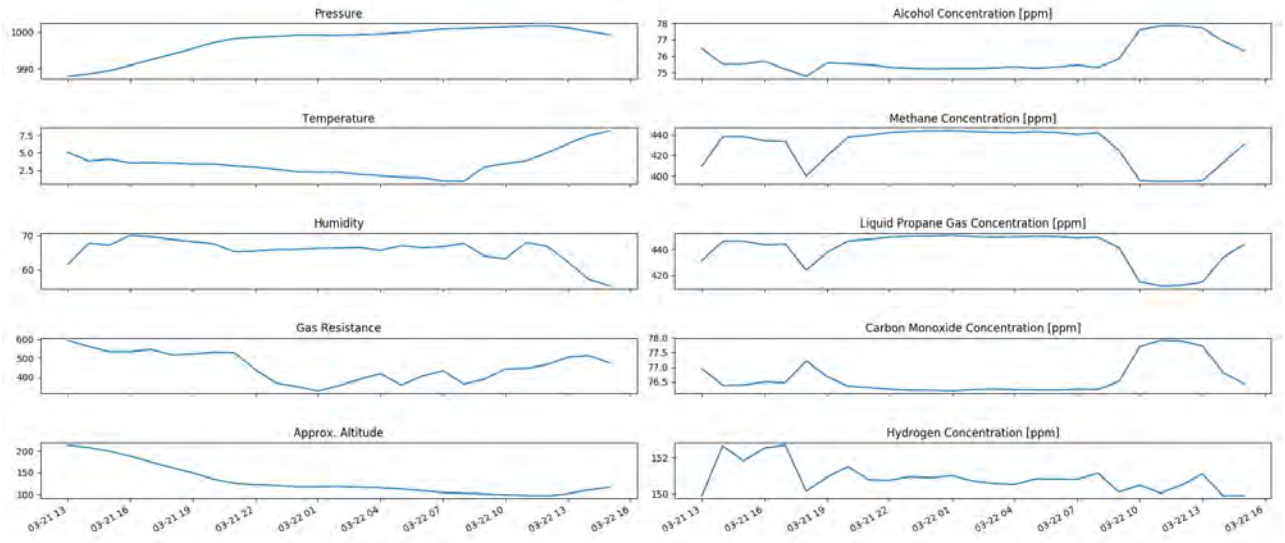

Figure 26: This figure displays data from a preliminary run in the open-air barn. The data is not calibrated, but the low selectivity of the sensors can be observed in the trends of the measurements. The synchronous responses of the oxidizing and reducing sensors, respectively, are clear. The increases in carbon monoxide concentration (seen near the beginning and at the end of the measurements) are likely due to the presence of a truck bringing feed into the barn, as they correlate well with the scheduled feeding times.(Klein, 2014)

8 Acknowledgments

We would like to thank Dr. Joshua McCann for his insightful comments and for putting us in contact with the Beef and Sheep Field Research Laboratory. We would also like to thank the Field Research Laboratory's farm manager, Miles Redden, who was kind enough to allow us access to the cattle, help us set up the devices, and offer advice on device placements. We would also like to thank his assistant Cody Dawson who was likewise extremely helpful in the conduction of this experiment. In addition, we extend our gratitude to Professor George Gollin, as well as teaching assistants Justin Languido and Christian Williams, for their advise and aid over the course of the semester.

References

Are cows the cause of global warming? 2008. URL https://timeforchange.org/are-cows-cause-of-global-warming-meat-methane-co2/.

Adafruit. Adafruit bme680 - temperature, humidity, pressure and gas sensor, 2019. URL https://www.adafruit.com/product/3660.

Arduino. Arduino mega 2560 rev3, 2019. URL https://store.arduino.cc/usa/mega-2560-r3.

Atmel. *Atmel ATmega640/V-1280/V-1281/V-2560/V-2561/V*, 2014.

Bosch. *BME680 - datasheet*, 7 2017.

US Environmental Protection Agency: EPA. Understanding global warming potentials. 2017. URL https://www.epa.gov/ghgemissions/understanding-global-warming-potentials.

US Environmental Protection Agency: EPA. Overview of greenhouse gases. 2019. URL https://www.epa.gov/ghgemissions/overview-greenhouse-gases.

Haoshuang Gu, Zhao Wang, and Yongming Hu. Hydrogen gas sensors based on semiconductor oxide nanostructures. *Sensors*, 12(5):5517–5550, 2012. ISSN 1424-8220. doi: 10.3390/s120505517. URL https://www.mdpi.com/1424-8220/12/5/5517.

D. E. Johnson K. A. Johnson. Methane emissions from cattle. *Journal of Animal Science*, 73(8): 2483—2492, 1995. URL "https://doi.org/10.2527/1995.7382483x".

Locke Klein. *40 maps that explain food in America*, 2014. URL https://www.vox.com/a/explain-food-america.

R.M. Negri. 6.3 - electronic noses in perfume analysis. In Amparo Salvador and Alberto Chisvert, editors, *Analysis of Cosmetic Products*, pages 276 – 290. Elsevier, Amsterdam, 2007. ISBN 978-0-444-52260-3. doi: https://doi.org/10.1016/B978-044452260-3/50037-1. URL http://www.sciencedirect.com/science/article/pii/B9780444522603500371.

Park T. Kim M. et al. Patra, A. Rumen methanogens and mitigation of methane emission by anti-methanogenic compounds and substances. *J Animal Sci Biotechnol*, 8(13), 2017. URL https://doi.org/10.1186/s40104-017-0145-9.

Alcohol Gas Sensor. Zhengzhou Winsen Electronics Technology Co., Ltd, 1.4 edition, 3 2015a. URL https://www.winsen-sensor.com/d/files/semiconductor/mq-3b.pdf.

Combustible Gas Sensor. Zhengzhou Winsen Electronics Technology Co., Ltd, 1.4 edition, 3 2015b.

Flammable Gas Sensor. Zhengzhou Winsen Electronics Technology Co., Ltd, 1.4 edition, 3 2015c. URL https://www.winsen-sensor.com/d/files/semiconductor/mq-6.pdf.

Semiconductor Hydrogen Gas Sensor. Zhengzhou Winsen Electronics Technology Co., Ltd, 1.4 edition, 3 2015d. URL https://www.winsen-sensor.com/d/files/semiconductor/mq-8.pdf.

Toxic Gas Sensor. Zhengzhou Winsen Electronics Technology Co., Ltd, 1.5 edition, 4 2018.